

# Measurements of level of rebar corrosion and surface cracking for structural health monitoring

S. Shakib & A.Z. Morshed

*Khulna University of Engineering and Technology, Khulna 9203, Bangladesh*

**ABSTRACT:** The very first visibly affected part of reinforced concrete members due to corrosion is the concrete cover, which is relatively much thinner than the core concrete. The deterioration caused by cracking and spalling of the cover concrete in bridges has been recognized as a serious serviceability issue and of the greatest maintenance challenges worldwide, especially in tropical coastal climatic regions of Bangladesh. This paper presents an experimental investigation on the prediction of level of corrosion by monitoring the initiation of surface crack, its width and propagation induced by expansive pressure from corrosion products. This information would be useful for structural health monitoring system of bridges exposed to marine environment. Level of corrosion has been measured in terms of mass loss ( $\text{mg}/\text{cm}^2$ ) and thickness of corrosion products around the reinforcement ( $\mu\text{m}$ ). Cylindrical plate having 100 mm- $\varnothing$  and 50 mm in thickness was used as test specimens. Corrosion was accelerated by using impressed current technique. The thicknesses of corrosion products accumulated around the reinforcement was measured through image analysis. A thickness of corrosion products of 50-73  $\mu\text{m}$  and corresponding mass loss of 20-22  $\text{mg}/\text{cm}^2$  was found to cause crack formation on the concrete cover and propagate inwards.

## 1 INTRODUCTION

Bangladesh is a riverine country with over 230 rivers flowing over the country (The Daily Prothom Alo, March 14, 2019). For uninterrupted communication system both in roads and railways, a lot of bridges have been constructed on the rivers. According to Roads and Highway Department (RHD), Bangladesh, there are 3548 nos. of bridges, 14814 nos. of culverts and 856 nos. of baily bridges all over the country. Among them about 21% bridges and 25% culverts are situated in the coastal region (Khulna and Chottogram) (RHD 2019). Budget allocated for maintenance of Bridges of Bangladesh for the past few years, as shown in Table 1, demonstrates that a huge costing was incurred for periodic maintenance of bridges, a major part of which originated due to corrosion.

Nowadays, structural health monitoring (SHM) has become an effective system for durability assessment (Shakib & Morshed 2019, Zhou & Jin 2016, Kulkarni & Achenbach 2008). This system is a combination of visual inspection and response of different reliable sensors, installed on the structure to monitor the progress of damage (Comisu et al. 2017). This system is capable of evaluating the serviceability condition, the reliability of the structure, and the remaining functionality in terms of durability (Comisu et al. 2017, Sousa et al. 2011).

Table 1. Maintenance budget for bridges in Bangladesh (RHD, 2018).

Budget item	Fiscal year (Million Taka)			
	2014	2015	2016	2017
Routine maintenance	750	800	950	1000
Periodic Maintenance Program minor (Road & Bridge)	2996	4307	3285	3739
Periodic Maintenance Program Major (Road)	8103	8080	8850	10600
Periodic Maintenance Program Major (Bridge)	1200	1350	1600	1500
Emergency Maintenance (Road & Bridge)	100	100	100	100
Total	13149	14637	14785	16939

SHM system comprises of five different operations; acquisition, validation, analysis, prognosis, and management of the system (Comisu et al. 2017). The system and the sensors are used to acquire parameters for the most important deterioration mechanisms: corrosion of reinforcement in bridges, carbonation of concrete, freeze-thaw cycles, alkali-silica reaction and mechanical damage, as well as the changes in the structures behavior and safety: static deformation, strains; crack widths and vibrations (frequencies, amplitudes, accelerations and vibration modes). In the coastal regions, chloride induced corrosion of reinforcement usually dominates over the carbonation of concrete and alkali-silica reaction. Freeze-thaw cycles may be negligible in Bangladesh.

Corrosion is an electrochemical process in which oxides of Iron in different forms are produced in the presence of suitable environment (Zhao & Jin 2016). Oxides are expansive in nature. They occupy 2-6 times larger volume than the parent material (Zhang & Poursaeed 2014). Due to the expansive nature of corrosion products, an outward pressure is generated on the surrounding concrete. Concrete cover is the most affected part due to this expansive pressure. The resultant tensile stress developed due to this pressure is released through the crack formation in the concrete, which is inherently weak to bear tensile stress. Generally, these cracks appear along the reinforcement which may be the first indication of the deterioration. The width of crack is dependent on the amount of mass loss of steel. In reality, direct measurement of mass loss of corroding steel embedded in the concrete members in an existing structure, is very difficult. Thus, indirect measurement for corrosion prediction is a more practicable approach for SHM. The width of crack at the surface of concrete could be one such parameter of importance for predicting the amount of corrosion. This prediction may help a lot to assess the risk of failure because of corrosion.

Previous studies showed that when the circumferential stress developed at the steel concrete interface due to the outward pressure, exceeds the tensile strength of concrete, crack initiated and propagated towards the concrete surface (Bhargava et al. 2006, El-Maaddawy & Soudki 2003, Pantazopoulou & Papoulia 2001, Val et al. 2009). On contrary, Shakib & Morshed (2019) observed that for a lower cover thickness, the surface of cover concrete heaved and crack initiated on the outer surface due to bending effect and then propagated inwards.

Available corrosion measurement techniques, such as half-cell potential measurement and linear polarization method are used to monitor only the state as well as rate of corrosion. But the level of corrosion may not be measured through these techniques. In this research, an experimental investigation was carried out to find the level of corrosion in terms of mass loss ( $\text{mg}/\text{cm}^2$ ) and the thickness of corrosion products around the reinforcement in relation with the surface crack width. Crack initiation and propagation pattern were also investigated.

## 2 EXPERIMENTAL PROGRAM

### 2.1 General

Impressed current technique was used to accelerate the corrosion of rebar. Thickness of corrosion products and the width of crack was measured by image analysis by capturing images on the top surface of the specimen using USB digital microscope at different time intervals. Mass loss was calculated using Faraday's law as following equation.

$$m_F = \frac{MIT}{ZF} \quad (1)$$

where,  $m_F$  = the mass loss of steel bars (gm),  $M$  = atomic weight of metal (For Fe,  $M = 56$ ),  $I$  = current (amperes),  $T$  = time (seconds),  $Z$  = ionic charge (for Fe,  $Z = 2$ ),  $F$  = Faraday's constant = 96,500 amperes/second.

### 2.2 Specimens

Concrete mix proportion designed according to ACI 211.1 is shown in Table 2. A w/c of 0.45 was selected to implement the codal restriction due to exposure condition of concrete in saline environment. ASTM Type-I (Ordinary Portland Cement) was used as binding material, 19 mm downgrade stone chips were used as coarse aggregate and river sand with fineness modulus of 2.8 was used as fine aggregate in concrete. The compressive strength and tensile strength of concrete was tested according to ASTM C39 and ASTM C426, respectively. The studied average compressive strength and tensile strength of concrete were found as 30 MPa and 2.9 MPa respectively.

Two types of steel reinforcement were used in this research. A 12 mm diameter Grade 60 MS plain bar was used to represent as anode and three 4 mm diameter wires were used as cathode. Length of each bar was 75 mm. The bar was coated by paint for a length of 25 mm so that the uncoated zone (surface area of 1885

mm<sup>2</sup>) may corrode in accelerated corrosion tests. The anode and cathode bars were embedded in a cylindrical concrete specimen of 100 mm in diameter and 50 mm thickness. The test specimen is shown in Figure 1. The 12 mm diameter bar (anode) was placed in the center of the specimen and three 4 mm diameter wires (cathode) were placed equidistant from each other as well as from central anode bar. It was assumed that, all the current is consumed to oxidize the steel in accelerated corrosion test. So that a certain amount of chloride ions is needed in the concrete. Before conducting the accelerated corrosion test the specimens were soaked at 3.5% NaCl solution for at least 1 day.

Table 2. Mix proportions for the concrete.

Materials (kg/m <sup>3</sup> )					w/c ratio
Water	Cement	Fine Aggregate	Coarse Aggregate	Fresh density	
190	422	677	1056	2345	0.45

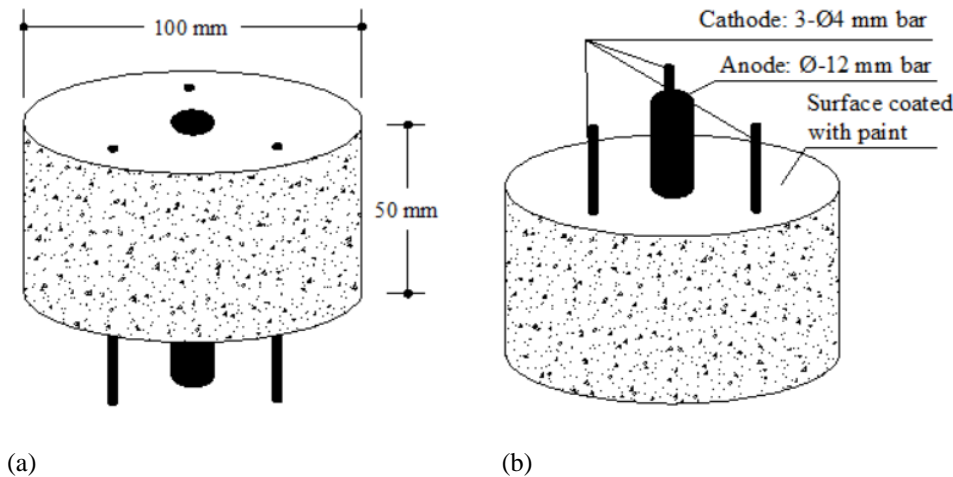


Figure 1. Details of specimen (a) top view (b) bottom view.

### 2.3 Tests Setup

In the electrochemical corrosion process a microcell is formed after the steel has depassivated and a potential difference is created between the corroding bar and the surrounding corrosion products which further accelerates the corrosion of steel. To simulate this phenomenon in a short time, an external DC power supply was used to apply a direct current between the anode (steel reinforcement) and cathode. The test setup is shown in Figure 2. A power supply of 30 V, 1 A was used. A constant voltage of 30 V was applied across the anode and cathode and the voltage drop across the fixed resistor was measured. From which the current supply was calculated by Ohm's law ( $I = V/R$ ). The top surface of the specimens was polished and smoothed with grade 400 sand paper and then cleaned with air blower and duster cloth. The bottom side of the specimen was sealed with epoxy paint before ponding it in 3.5% NaCl solution in such a manner that the chloride ions could penetrate only through the side surface. The thickness of corrosion product layer and crack width were observed by a magnifying USB digital Microscope, shown in Figure 3. The top surface of the specimens was dried and cleaned again before taking each photograph.

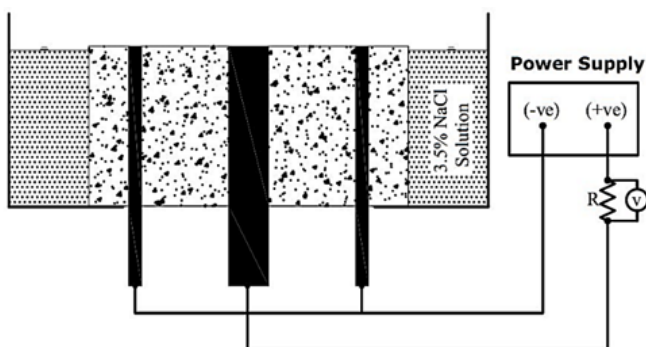


Figure 2. Details of test setup.



Figure 3. USB digital microscope.

### 3 RESULTS AND DISCUSSION

#### 3.1 Thickness of Corrosion Products

Color photographs, taken by the magnifying USB digital Microscope, could clearly illustrate the layer of corrosion products and the cracks formed due to expansive nature of corrosion products. The variation of thickness of corrosion products with respect to mass loss, as shown in Figure 4, demonstrates that up to about 8 mg/cm<sup>2</sup> of mass loss, layer of corrosion products was not significantly identifiable. It seems that during that time the corrosion products mostly diffused into the micro pores of the surrounding concrete. After this level of corrosion, layer of corrosion products became visible. At a level of corrosion of 20-22 mg/cm<sup>2</sup>, first crack was visible at about corrosion product thickness of 50-73 μm. Figure 4 also shows that the corrosion product thickness follows an approximately linear relationship with the level of corrosion. Nossoni and Harichandran (2014) also found a linear relation between them up to the first visible crack. In the process of corrosion, the parent material just converted to its oxides and accumulated around it. Since no products could be losses because of having surrounding concrete, it is logical to build the corrosion products linearly around the reinforcement.

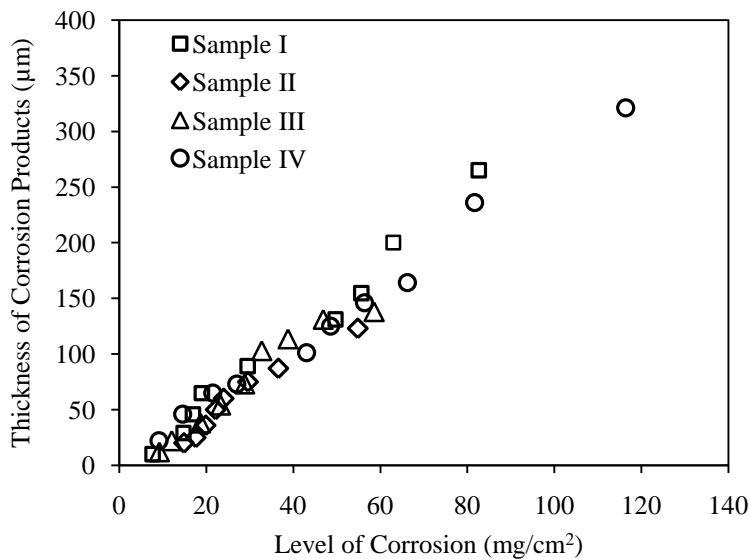


Figure 4. Variation of thickness of corrosion products against level of corrosion.

Time to cracking is very much dependent on the quality of concrete, bar diameter and concrete cover thickness (Liu & Weyers 1998, Bhargava et al. 2006, Bazant 1979, Dagher&Kulendran1987, Vidal et al. 2004, Maadway & Soudki 2007, Andrade et al. 1993). Dependency of these factors on first crack appearance by other researchers are tabulated in Table 3 and compared with the present study. Andrade et al. (1993) and Nossoni et al. (2014) reported a lower value of mass loss ( $\leq 10\text{mg/cm}^2$ ) needed to crack formation. Alonso et al. (1998) showed that the level of corrosion increased with increase in the cover thickness. However, Shakib et al. (2019) reported approximately similar level of corrosion (21-22 mg/cm<sup>2</sup>) needed to crack formation for a clear cover of 20 and 37.5 mm and observed that crack initiated at the cover surface first and then propagated inward. In this investigation, a level of corrosion of 20-22 mg/cm<sup>2</sup> was found to crack formation which is very similar to Shakib et al. (2019), Cabrera et al. (1996), El-Maadway et al. (2003) and Alonso et al. (1998). Thickness of corrosion products at crack formation was found as 50-73 μm. This value is slightly higher in comparison to that reported by Nossoni et al. (2014). This variation might be owing to variation in cover thickness, concrete quality and the rate of corrosion applied to accelerate the corrosion.

#### 3.2 Cracking of Cover Concrete

With an increase in the amount of corrosion products, a visible crack is initiated from the concrete surface and propagated towards the reinforcement. This phenomenon was also observed in beam specimen for cover of 20 mm and 37.5 mm (Shakib & Morshed 2019) and 30 mm (Tran et al. 2011). This may be due to the bending of the surface (Shakib & Morshed 2019) or cylindrical shape effect. The surface crack width was measured by image analysis. Figure 5 (a) shows one of test specimens with cover cracking. Images were captured by USB microscope are shown in Figure 5 (b) and 5 (c). In Figure 5 (a), a photograph is shown representing the major

crack formed through the cover concrete. The figure clearly shows the crack pattern. The magnified photograph of major crack at the cover surface is shown in Figure 5 (b). Another photograph is shown in Figure 5 (c) representing the layer of corrosion products.

Table 3. Comparison of results with other researchers.

Reference	Bar Dia (mm)	Concrete Cover (mm)	Concrete Strength (MPa)	Current Density ( $\mu\text{A}/\text{cm}^2$ )	Time to Appear First Crack (hr)	Level of Corrosion ( $\text{mg}/\text{cm}^2$ )	Thickness of Corrosion Products ( $\mu\text{m}$ )
Andrade et al.	16	20	24.0	100	96	10	--
Cabrera and Ghoddoussi	12	69	54.0	244	108	28	--
Alonso et al.	16	20	24.0	100	113	12	--
	16	50	24.0	100	208	22	--
	16	70	24.0	100	264	28	--
	16	70	24.0	10	2643	28	--
	12	50	24.0	100	350	37	--
El Maaddawy & Soudki	16	33	39.0	150	95	15	--
Shakib and Morshed	12	20	30.0	1000-1200	--	22.7	--
	12	37.5	30.0	1000-1200	--	21.2	--
	12	50	30.0	1000-1200	--	129	--
	12	75	30.0	1000-1200	--	211	--
Nossoni and Harichandran	12	12	57.2	4500	0.75-1	0.4	12-14.2
		20	57.2	4500	1.08-1.33	5	14-21
		31	57.2	4500	1.58-2.08	7	23-33
Author	12	44	30.0	2800	5.6-9.4	20-22	50-73

Figure 6 shows the variation of crack width with respect to the level of corrosion. The surface crack width varied linearly with the level of corrosion. The products due to corrosion, accumulated linearly around the re-bars, as shown in Figure 4, resulted in a linearly increased outbound pressure applied on the cover concrete. For this reason, the surface crack increased linearly due to this outbound pressure. The outbound pressure generated due to the expansive corrosion products released through crack formation. Normally clear cover is the shortest distance to be released. So that the cover concrete is the first affected part of the structure exposed to marine environment. On the other hand, the crack appeared on the surface was found to form along the reinforcement as shown in Figure 5(a). The cracks found on the surface maintaining this pattern can be easily monitored for reinforced concrete structures like bridges. Since the surface crack width maintained a linear relationship with the level of corrosion, this linear relationship between surface crack width and level of corrosion can be an effective tool for corrosion prediction.

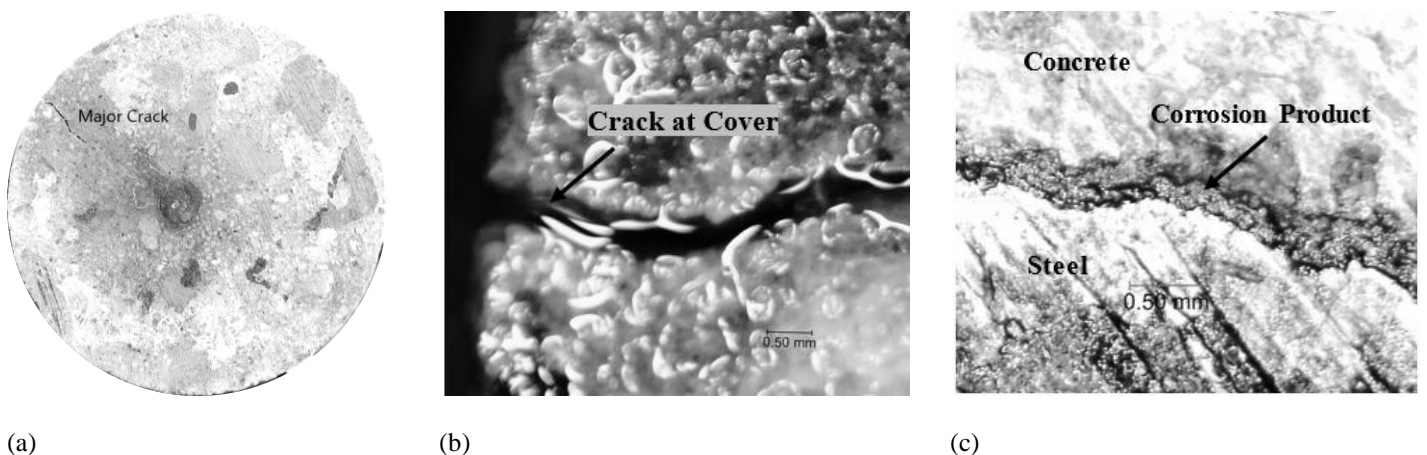


Figure 5. Crack pattern of the specimen (a) cylindrical plate specimen (b) crack mouth opening at cover (c) corrosion product build up at steel concrete interface.

For monitoring the structural health exposed to marine environment, level of corrosion of rebars is a key factor. Because the accumulation of corrosion products destroy the bond between rebars and surrounding concrete (Kearsley & Joyce 2014, Al-Sulaimani et al. 1990, Chung et al. 2004) consequences the reduction of flexural capacity of structures (Almusallam et al. 1996). Prediction of corrosion level by monitoring the sur-

face crack width can be effectively used in structural health monitoring system of corrosion prone structures specially Bridges.

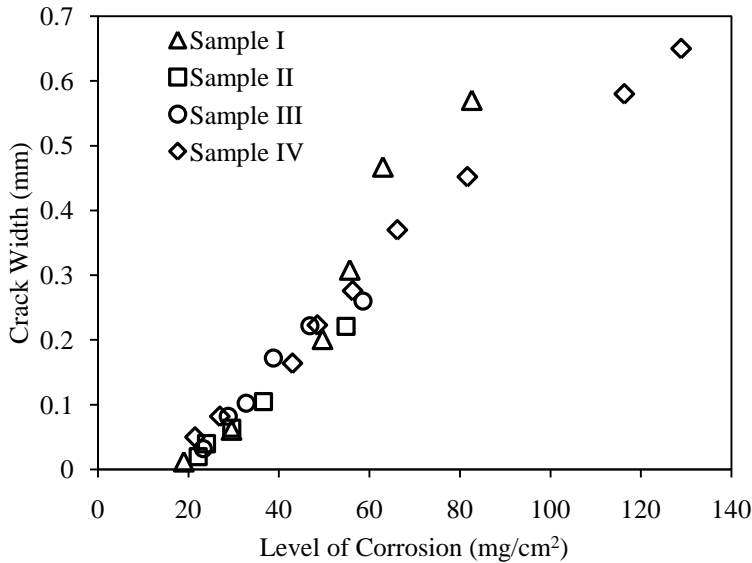


Figure 6. Surface crack propagation.

#### 4 CONCLUSIONS

Bridges are one of the most vulnerable structures in the coastal regions. In order to monitor the structural health of bridges exposed to corrosive environment, continuous assessment of mass loss of rebars is the key factor. Surface cracking is the first indication of cover failure. In this research, prediction technique of rebar corrosion was investigated by monitoring this surface cracks. It was found that the level of corrosion maintained a linear relationship with the surface crack width. Level of corrosion was measured in terms of mass loss as well as width of corrosion products accumulated around the rebars. It was also found that the crack was initiated at the cover surface and propagated towards the rebar. A thickness of corrosion products of 50-73  $\mu\text{m}$  and corresponding mass loss of 20-22  $\text{mg}/\text{cm}^2$  was found to cause crack formation on the concrete cover.

#### REFERENCES

- Almusallam, A. A., Gahtani, A. S. A., Aziz, A. R., Dakhil, F. H. & Rasheeduzzafar. 1996. Effect of reinforcement corrosion on flexural behavior of concrete slabs. *Journal of Materials in Civil Engineering*, 8(3).
- Alonso, C., Andrade, C., Rodriguez, J. & Diez, J. M. 1998. Factors controlling cracking of concrete affected by reinforcement corrosion. *Materials and Structures* 31(7): 435-441.
- Al-Sulaimani, G. J., Kaleemullah, M., Bassunbul, I. A. & Rasheeduzzafar. 1990. Influence of corrosion and cracking on bond behaviour and strength of reinforced concrete members. *ACI Structural Journal* 87(2): 220-231.
- Andrade, C., Alonso, C. & Molina, F. J. 1993. Cover cracking as a function of bar corrosion: part I-experimental test. *Materials and Structures* 26(8): 453-464.
- Bazant, Z. P. 1979. Physical model for steel corrosion in concrete sea structures—theory. *Journal of the Structural Division* 105(6): 1137-1153.
- Bhargava, K., Ghosh, A. K., Mori, Y. & Ramanujam, S. 2006. Model for cover cracking due to rebar corrosion in rc structures. *Engineering Structures* 28(8): 1093-1109.
- Cabrera, J. G. 1996. Deterioration of concrete due to reinforcement steel corrosion. *Cement and Concrete Composites*, 18(1): 47-59.
- Chung, L., Cho, S., Kim, J. J. & Yi, S. 2004. Correction factor suggestion for ACI development length provisions based on flexural testing of RC slabs with various levels of corroded reinforcing bars. *Engineering Structures*, 26: 1013-1026.
- Comisu, C., Taranu, N., Boaca, G. & Scutaru, M. 2017. Structural health monitoring system of bridges. *X International Conference on Structural Dynamics, EURO DYN 2017, Procedia Engineering* 199:2054-2059.
- Dagher, H. J., & Kulendran, S. 1987. Finite element modeling of corrosion damage in concrete. *ACI Structural Journal*, 89(6)
- El-Maaddawy, T. A. & Soudki, K. A. 2003. Effectiveness of impressed current technique to simulate corrosion of steel reinforcement in concrete. *Journal of Materials in Civil Engineering* 15(1): 41-47.
- He, J., Zhou, Y., Guan, X., Zhang, W., Wang, Y., & Zhang, W. 2016. An integrated health monitoring method for structural fatigue life evaluation using limited sensor data. *Materials (Basel, Switzerland)*, 9(11).

- Kearsley, E. P. & Joyce, A. 2014. Effect of corrosion products on bond strength and flexural behaviour of reinforced concrete slabs. *Journal of the South african institution of civil engineering* 56(2):21–29
- Kulkarni, S. S. & Achenbach, J. D. 2008. Structural health monitoring and damage prognosis in fatigue. *Structural Health Monitoring* 7(1): 37–49.
- Liu, Y. & Weyers, R. E. 1998. Modeling the time-to-corrosion cracking in chloride contaminated reinforced concrete structures. *ACI Materials Journal* 95(6): 675–680.
- Nossoni, G. and Harichandran, R. S. 2014. Electrochemical-mechanistic model for concrete cover cracking due to corrosion initiated by chloride diffusion. *Journal of Materials in Civil Engineering* 26(6).
- Pantazopoulou, S. J. & Papoulia, K. D. 2001. Modeling cover-cracking due to reinforcement corrosion in rc structures. *Journal of Engineering Mechanics* 127(4): 342–351.
- Shakib, S. & Morshed, A. Z. 2019. Experimental investigation on crack initiation and propagation due to corrosion of reinforcement. *Advances in Civil Engineering Materials* 8(1): 688-698
- Sousa, H., Félix, C., Bento, J. & Figueiras, J. 2011. Design and implementation of a monitoring system applied to a long-span prestressed concrete bridge. *Structural Concrete* 12(2):82-93
- Tran, K. K., Nakamura, H., Kawamura, K. & Kunieda, M. 2011. Analysis of crack propagation due to rebar corrosion using RBSM. *Cement and Concrete Composites* 33(9): 906–917.
- Val, D. V., Chernin, L. & Stewart, M. G. 2009. Experimental and numerical investigation of corrosion-induced cover cracking in reinforced concrete structures. *Journal of Structural Engineering* 135(4): 376–385.
- Vidal, T., Castel, A. & François, R. 2004. Analyzing crack width to predict corrosion in reinforced concrete. *Cement and Concrete Research* 34(1): 165–174.
- Zhang, Y., & Poursaeed, A. 2014. Study the passivation and corrosion activity of carbon steel in concrete simulated pore solution under tensile and compressive stresses. *ASCE Journal of Materials in Civil Engineering*, 4014234
- Zhao, Y. & Jin, W. 2016. Steel corrosion-induced concrete cracking. *China Science Publishing & Media Ltd.*